Intra- and Intermolecular Packing in Polyolefin Blends

Arun Neelakantan and Janna K. Maranas*

Department of Chemical Engineering, The Pennsylvania State University, University Park, Pennsylvania 16802

Received July 9, 2003; Revised Manuscript Received December 10, 2003

ABSTRACT: The response of chain packing for four saturated hydrocarbon polymers, poly(ethylene−propylene), poly(ethylene−butene), isotactic polypropylene, and head-to-head polypropylene, to changes in environment are considered. The changes arise from mixing each material with the three others in the series. Intra- and intermolecular packing are considered separately by using molecular dynamics simulation, where unambiguous separation of the two is possible. We assess changes from the pure state in chain dimensions [radii of gyration and end-to-end distances], the intramolecular pair distribution functions, and the intermolecular pair distribution functions of each component [the A/A and B/B distributions]. Although it cannot be compared to the melt, the cross [A/B] intermolecular pair distribution function is also considered. We find that chain dimensions and intramolecular packing are insensitive to mixing. Regardless of the nature of the second component, these quantities are invariant within our ability to measure them. In contrast, intermolecular packing changes considerably on mixing. The changes are not energetically driven; i.e., the packing differences do not cause a favorable energetic response in the system. Of the six possible mixtures considered, two appear athermal, one has a preference for A/B contacts, two have decreased A/B contacts, and one changes only slightly from the pure component distributions.

I. Introduction

A defining feature of polymer melts and blends on length scales less than 1.5 nm is the local arrangement of neighboring chain segments. This arrangement can be characterized by the intermolecular pair distribution function, which measures the local density of intermolecular contacts relative to the bulk density as a function of separation distance. For some polymers, a peak is found that characterizes the preferred nearest chain packing distance, while others are completely void of such preferences. Small changes in local chain architecture give rise to these differences. For example, within the series of saturated hydrocarbon polymers—polypropylene [PP], head-to-head polypropylene [hhPP], and poly(ethylene−propylene) [PEP]—the local chain architecture changes from a methyl group placed on every second backbone carbon [PP] to every fourth backbone carbon [PEP]. As a result, the intermolecular pair distribution function, $g^{\text{inter}}(r)$, changes from a featureless curve to one showing a significant preference for nearest chain placement at $\sim$5.5 Å^{-1}. This ordering affects both thermodynamic and dynamic properties, for example, the cohesive energy density[2] and structural relaxation on short time scales.[3,4]

Our previous work has characterized intermolecular packing in polyolefin melts using the molecular dynamics method.[1,2,5] The choice of this method for characterizing intermolecular packing is due to the difficulty in separating intermolecular from intramolecular contributions in appropriate experimental methods, such as neutron diffraction. Possibilities for such a separation include neutron diffraction isotopic substitution experiments,[6] in which it is possible to obtain the intermolecular hydrogen−hydrogen distribution of a polymer in the melt state, and reverse Monte Carlo simulation,[7] where the coordinate positions of all atoms are generated to describe a measured diffraction pattern. We are not aware of extension of either method to isolate the intermolecular distribution of a single polymer in a blend. Packing in polyolefin melts has been addressed using simulation[1,2,5,8−12] and the liquid state theory PRISM.[13−17] All these results show that although intermolecular packing in polyolefins is universal on length scales of R_g and greater, at short distances, intermolecular packing varies significantly as a function of pendant group spacing and size, as mentioned above. The most important factor is the pendant group spacing. If the pendant group spacing is low as in polypropylene, preferential packing of chains is prevented. As the pendant group spacing increases, packing is enhanced. A secondary factor is the pendant group size. Packing is decreased as the size of the pendant group is increased, but the size of the effect is smaller than that of pendant group spacing. In addition to the molecular dynamics results discussed above, these trends have been observed in a systematic study of pendant group spacing and size using PRISM.[17]

Here we extend our melt results to consider all possible mixtures of poly(ethylene−butene) [PEB], poly(ethylene−propylene) [PEP], isotactic poly(propylene) [PP], and head-to-head poly(propylene) [hhPP]. The repeating units of these systems are given in Figure 1. Also included in the figure are minority structures [$\sim$7% of repeat units] in PEP and PEB that arise from anionic polymerization of these materials. We have found that including these minority structures improves correspondence between simulated and experimental data.[2] Five of the six combinations show miscibility[18] and have various degrees of conformance to the solubility parameter formalism, in which the Flory interaction parameter is proportional to the difference in solubility parameters of the pure components.[19] In particular, the PEP−PEB blend is the only homopolymer−homopolymer blend that conforms to this simple theory. In a previous contribution, we investigated packing in mixtures of random ethylene−butene copolymers.[20] These will be noted as EB copolymers in the discussions below. In that study, most of the mixtures behaved athermally,

10.1021/ma0303770 CCC: $27.50
Published on Web 10/01/2004

poly(ethylene butene) – [PEB]

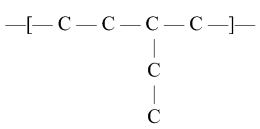

PEB – Minority structure

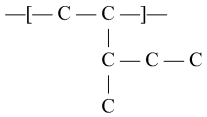

poly(ethylene propylene) – [PEP]

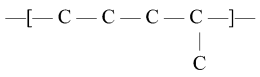

PEP – Minority structure

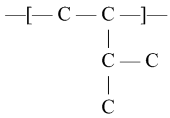

isotactic poly(propylene) – [PP]

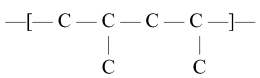

head-to-head poly(propylene) – [hhPP]

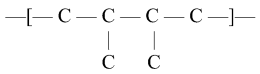

Figure 1. Repeat units of all materials. Hydrogen atoms are omitted for clarity.

but there were exceptions relating to a geometric incentive for packing efficiency.

II. Background

Packing in Polymer Blends. In an A/B blend, there are three relevant distributions: A−A, B−B, and A−B. The mixture results we present here focus on changes in the A−A and B−B distributions from the melt state when mixed with various second components. We also consider the A−B or cross-correlation. An overview of packing in mixtures was given in ref 20, and the reader is referred there for additional information. Of relevance here is the behavior of athermal [purely repulsive] blends,[21−23] where the component with the most ordering, or the stiffer component, becomes more ordered on mixing, while that which packs least efficiently in the melt becomes even less ordered. The cross-correlation A−B closely follows either the geometric or arithmetic combining rules. We also mention that blends of polyolefins that have been specifically addressed include PIB/hhPP,[24] PE/hhPP,[25] polypropylenes of varying tacticities [sPP/iPP, iPP/aPP, and aPP/sPP],[26] and PE/iPP.[27] The PE/hhPP and PE/iPP blends are immiscible, with both the A/A and B/B distributions showing like species clustering. For the polypropylene blends, in iPP/aPP little change in either of the intermolecular distributions is observed, whereas both iPP/sPP and aPP/sPP have enhanced self-packing and low A/B correlation with the effect larger for iPP/sPP. This is again consistent with immiscibility.

Table 1. Blend Densities Used as Simulation Input

blend	density (g/cm^3)	blend	density (g/cm^3)
HHPP−PEP	0.7702	PEP−PEB	0.7696
HHPP−PEB	0.777	PEP−PP	0.7624
HHPP−PP	0.7698	PP−PEB	0.7692

In the six blends we consider, two behave athermally, and one opposite of athermal—its distributions move closer together in the blend, one has a preference for A/B contacts, and two have decreased A/B contacts. These results show larger variation than our EB copolymer study, where 8 out of 10 blends were athermal, and suggest that athermal behavior may be characteristic of "regular mixing", the term given to blends that follow the solubility parameter formalism.

III. Simulation Methods

A. Model. The model is an extension of the optimized force field for liquid hydrocarbons [OPLS] introduced by Jorgensen et al.[28] The united atom method is used, which models each carbon atom collectively with the hydrogen atoms to which it is bonded: CH, CH_2, and CH_3. For static properties of polyethylene melts, differences between united atom models and models where hydrogen atoms are explicitly modeled are small.[29,30] The polyolefins in the current work have also been tested against comparable explicit atom models with comparable performance for thermodynamic and structural properties.[31] Constraint forces on each united atom represent covalent bonds, maintaining a fixed carbon−carbon bond length of 1.54 Å. Bonded interactions are taken into account through bending and torsional potentials, while Lennard-Jones (LJ) interaction sites located at the center of mass of each united atom characterize nonbonded interactions. A full discussion of the model, including bonded and nonbonded parameters, can be found in ref 2. The equations of motion were integrated by means of the velocity Verlet algorithm[32] using a time step of 5 fs, and the bond length was kept constant using the RATTLE algorithm.[32]

The initial configurations for all the systems considered in this study were generated as described by Mondello et al.[32] Each type of chain is first generated in an all-trans configuration. Multiple copies of the required chains for each blend are placed in a cubic MD cell, whose size is sufficiently large to ensure that none of the chains overlap. The MD program is run to allow the chain to relax, and at the same time the box size is gradually reduced to the desired value [governed by the density of the material]. Relevant trans/gauche ratios were quickly established [within ∼40 ps], so that the system has no memory of the imposed initial state. All simulations are run with a system of 50 molecules and at a temperature of 150 °C. A constant temperature is maintained using the velocity rescaling algorithm of Berendsen et al.[33] The blends are 50% mixtures, containing 25 chains of A and 25 chains of B. Each chain consists of 62 united atoms. The selection of this chain length results from the intermolecular $g(r)$ stabilizing around this molecular size—at smaller molecular sizes, slight differences are observed, but further increases lead to little change. The blend densities are set by neglecting volume changes on mixing, as in general, these changes are small for polyolefin blends.[34] The blend density is then $\rho_{blend} = (\rho_A + \rho_B)/2$, where the ρ_i for 62 carbon chains are determined from their polymer counterparts as described in ref 3. The resulting densities ρ_{blend} used in the simulation are given in Table 1.

B. Calculated Quantities. Cohesive Energy Density. The cohesive energy density (CED) is defined as the energy of vaporization per unit volume:

$$\mathrm{CED} = \frac{U_G - U_L}{V_L} \cong \frac{-U_{inter}}{V_L} \tag{1}$$

Here we approximate the energy of vaporization with the intermolecular energy as shown in the second equality.

Pair Distribution Functions. The pair distribution functions are given by

$$[g(r)]_{inter} = \frac{\langle \rho(r')[\rho(r'+r)]_{inter} \rangle}{\langle \rho(r')_{inter} \rangle^2} \tag{2}$$

$$[g(r)]_{intra} = \frac{\langle \rho(r')[\rho(r'+r)]_{intra} \rangle}{\langle \rho(r')_{intra} \rangle^2} \tag{3}$$

in which $\rho(r')$ and $\rho(r'+r)$ are the instantaneous densities of united atoms at the locations r' and $r'+r$. The subscript "inter" in eq 2 indicates that the only pairs where the two united atoms belong to different chains are counted. Similarly, the subscript "intra" in eq 3 requires pairs where the two united atoms are on the same chain. The angular brackets indicate averages of all r' locations of united atoms in the simulation box, with $\langle \rho(r') \rangle$ equal to the macroscopic density. The implementation of these formulas in determining the distributions from simulation coordinates, including the normalizations appropriate for A/A, B/B, and A/B distributions in blends, has been described previously.[20]

Chain Dimensions and Time-Dependent Functions. To assess changes in chain dimensions with mixing, we determine the radius of gyration (R_g) and end-to-end distances (R_e) of the pure components and each component in the blends. The radius of gyration is determined using

$$R_g = \left\langle \sqrt{\frac{\sum_i m_i (\mathbf{r}_i - \mathbf{r}_{CM})^2}{M}} \right\rangle \tag{4}$$

The summation is taken over the N united atoms in a chain [total mass M, united atom mass m_i], and the average is taken over the chains of each type separately and over many coordinate snapshots. Thus, from one mixture we obtain R_g^A and R_g^B. The $\mathbf{r}_i$ are the positions of united atom i and the center of mass $\mathbf{r}_{CM}$ of each chain is $\mathbf{r}_{CM} = (\sum_i m_i \mathbf{r}_i / M)$. Similarly, the end-to-end distance

$$R_e = \langle |(\mathbf{r}_1 - \mathbf{r}_n)| \rangle \tag{5}$$

where $\mathbf{r}_1$ and $\mathbf{r}_n$ are the positions of the first and last united atoms on a chain, is also averaged over all chains of each type and many coordinate snapshots, yielding R_e^A and R_e^B.

In determining appropriate equilibration times, we use the mean-square displacement:

$$\mathrm{msd}(t) = \langle |\mathbf{r}(t) - \mathbf{r}(0)|^2 \rangle \tag{6}$$

where $\boldsymbol{r}(t)$ is the position of an atom at time t. This calculation is also made for each blend component separately.

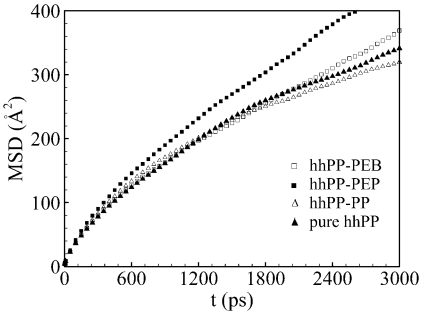

Figure 2. Mean-square displacement for hhPP in the melt and in blends. Symbols are as in the figure legend.

C. Equilibration and Model Assessment. The criterion we use to assess equilibration in each system is that the mean distance moved by the united atoms is greater than $2R_g$. The mean distance is determined from the mean-square displacement of both blend components. Mean-square displacements are shown in Figure 2 for pure hhPP, the slowest of the four materials, and hhPP in PEP, PEB, and PP. The latter three cases are denoted by hhPP−PEP, hhPP−PEB, and hhPP−PP in the figure legend. The data shown begin after the final density [box size] is reached. The R_g for hhPP [~9.4 Å] is insensitive to mixing, and so the united atoms require 2.0 ns [hhPP in PEP] to 3.0 ns [hhPP in PP] to move $2R_g$. We have set an equilibration time of 3 ns for all materials, which is the time required the slowest moving of our systems. In this time, the end-to-end vector autocorrelation function decays to 0.20 or less for all components in all blends. Mixing results in enhanced or inhibited mobility depending on the host. Further results on the effects of mixing on dynamics will be presented in a forthcoming publication.

Following equilibration, data acquisition runs of 1.5 ns were performed for all systems, with coordinate dumps every 2.5 ps. The radial distribution functions were then calculated as averages over every 500 ps and monitored for drifts that may indicate further equilibration is necessary. No such drifts were detected. The distribution functions for mixtures have larger variations than the pure components. Since the equilibration criteria used for mixtures were identical to the pure components, the larger variations do not indicate that the mixtures are further from equilibrium, but rather result from concentration fluctuations present in mixtures, but not in pure components. Other authors have noted similar observations.[35]

The model has been tested for a variety of polyolefins against experimental data for thermodynamic properties,[36] chain packing,[37] chain dimensions,[3,20] and dynamics[3] in the form of incoherent and coherent neutron scattering and NMR relaxation times. In all cases, the model is able to correlate the experimental data quite well, particularly the changes that occur as the chemical structure of the repeat unit is varied.

IV. Results and Discussion

Intramolecular Packing. In this section, we present our results on the influence of environment, as manipulated by mixing with various second components, on the packing of PP, hhPP, PEP, and PEB. We consider intramolecular and intermolecular packing separately, as they have very different responses to mixing. To characterize intramolecular packing, we consider changes in chain dimensions, R_g^i and R_e^i, with mixing and the

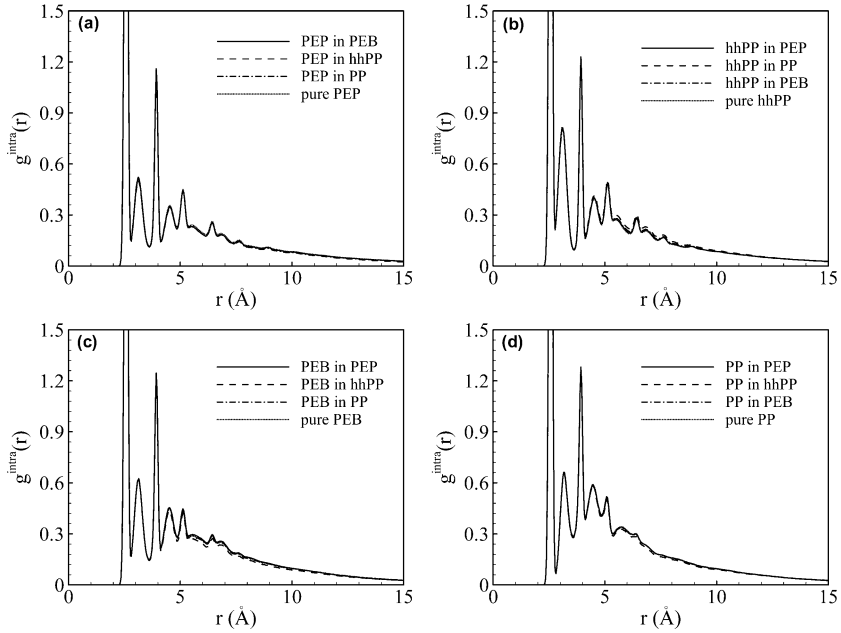

Figure 3. Influence of environment on intramolecular packing. The intramolecular pair distribution functions for each material are shown in the melt and in blends with the other three materials. (a) PEP, (b) hhPP, (c) PEB, and (d) PP. Symbols are as in the figure legend.

Table 2. Chain Dimensions as a Function of Mixing

polymers	R_g (Å)	R_e (Å)	polymers	R_g (Å)	R_e (Å)
PEP	9.8 ± 0.2	23.6 ± 2.2	hhPP	9.3 ± 0.1	23.1 ± 0.6
PEP in PP	10.1 ± 0.2	26.0 ± 1.2	hhPP in PP	8.9 ± 0.1	21.9 ± 0.5
PEP in hhPP	10.1 ± 0.2	25.4 ± 1.0	hhPP in PEB	9.2 ± 0.2	22.6 ± 0.7
PEP in PEB	10.2 ± 0.3	24.6 ± 1.1	hhPP in PEP	9.3 ± 0.3	23.4 ± 0.9
PEB	8.5 ± 0.2	20.3 ± 0.8	PP	8.1 ± 0.1	19.9 ± 0.4
PEB in PP	8.4 ± 0.2	20.0 ± 0.9	PP in hhPP	8.4 ± 0.1	21.5 ± 0.9
PEB in hhPP	8.6 ± 0.3	21.4 ± 2.0	PP in PEB	8.0 ± 0.2	19.4 ± 0.7
PEB in PEP	8.4 ± 0.2	21.0 ± 1.2	PP in PEP	8.0 ± 0.2	19.4 ± 1.1

intramolecular pair distribution functions $g^{intra}(r)$. The chain dimensions of each component, both in the pure state and when blended with the remaining three, are given in Table 2. From these results it is apparent that both radii of gyration and end-to-end distances are insensitive to mixing. This suggests that the response of single chain configurations to mixing is negligibly small. We have examined the response of local intramolecular configuration, as opposed to whole chain configuration, to mixing by considering the intramolecular distribution functions. These functions for all materials, both in their pure state and in the three other components with which they were mixed, are shown in Figure 3. The figure appears to show a single curve because all four curves coincide. Thus, as with chain dimensions, the packing of united atoms within a single chain does not change when that chain is placed in a different environment. This is true not only for small distances that reflect the bond bending and torsion angles that are most favored but also at larger length scales that are indicative of the placement of one chain end relative to the other. The same behavior was observed for all 10 ethylene−butene copolymer blends we have investigated.[20]

Intermolecular Packing. The situation is quite different for intermolecular packing. The response of the intermolecular pair distribution function, $g^{inter}(r)$, of each material to the three different environments afforded by blending is illustrated in Figure 4. For each blend, we consider three distributions: A/A, B/B, and A/B. For example, in the PEP/PP blend, PEP/PEP, PP/PP, and PEP/PP distributions are determined. Each part of Figure 4 represents the response of one component [A for example] to blending with the other three, i.e., the A/A distribution in each blend. Figure 4a represents PEP, and thus the PEP/PEP distributions [labeled PEP in X] are shown for each of the three second components, along with the PEP/PEP distribution in pure PEP. Similarly, hhPP/hhPP, PEB/PEB, and PP/PP distributions are shown in the remainder of the figure. The cross-distributions, PEP/PP for example, will be considered below. Before turning our attention to the influence of environment on the packing of each material, as reflected in the figure, we review our observations on the influence of environment from the EB copolymers.[20] In that study, materials that pack well in their pure state, i.e., $g^{inter}_{pure}(r)$ is highly structured, were more resistant to altering than packing when mixed. Shifts in $g^{inter}(r)$ away from $g^{inter}_{pure}(r)$ were typically such that the efficient packers become even more efficient when mixed with poor packers and vice versa; i.e., the distributions move further apart on blending. This is characteristic of athermal systems.[21−23] The size of these shifts was related to the difference in packing characteristics of the blend two components: blends of components with similar $g^{inter}_{pure}(r)$ changed the least.

With the exception of PP, these observations apply here as well. We first consider the propensity of the materials to alter their intermolecular packing when mixed. The efficiency of packing for the pure components, as assessed by the height of the first peak in

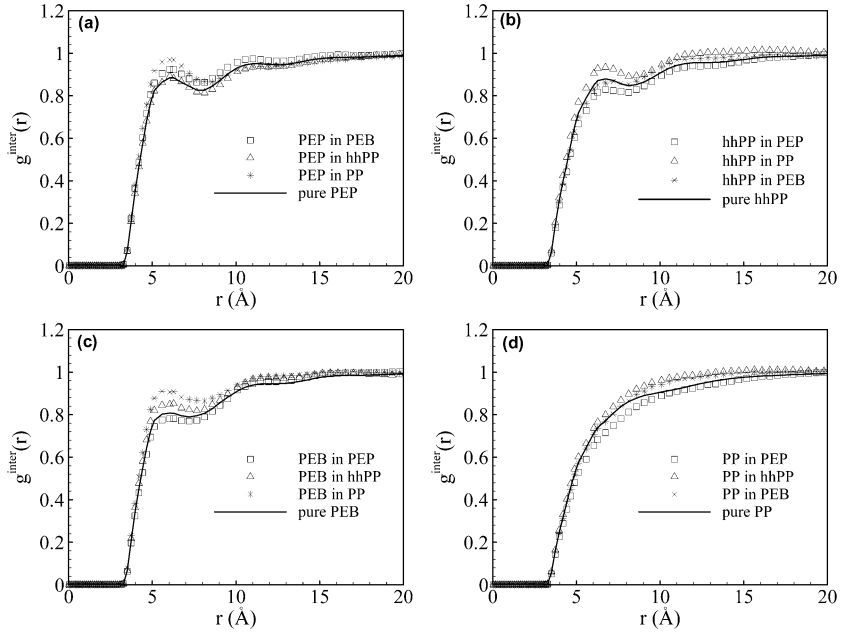

Figure 4. Influence of environment on intermolecular packing. The A/A or self-intermolecular pair distribution functions for each material are shown in the melt and in blends with the other three materials. (a) PEP, (b) hhPP, (c) PEB, and (d) PP. Symbols are as in figure legend.

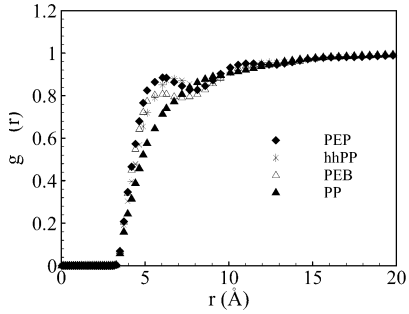

Figure 5. Intermolecular packing of all materials in the melt. Symbols are as in the figure legend.

$g^{inter}(r)$, follows the order PEP > hhPP > PEB > PP, as illustrated in Figure 5, where the four pure component distributions are plotted together. Figure 4 is presented in order of decreasing packing efficiency. Figure 4a is for the most ordered material, PEP, and Figure 4d is for the least ordered material, PP. Comparing the response of the PEP/PEP, hhPP/hhPP, and PEB/PEB distributions (Figure 4a−c) to mixing, an increase in the spread of the distributions is noticeable as packing efficiency decreases. For the efficient packer PEP, variations in the PEP/PEP distribution with environment are less than those for PEB, which does not pack as efficiently. The exception to this trend is PP (Figure 4d), where the spread in PP/PP distributions is similar to PEP, although it is the least efficient packer of the series.

The direction of shifts in $g^{inter}(r)$ with mixing is most often such that distributions in the blend are further separated than pure component distributions, as in athermal mixtures. This implies that the more structured of the two components will become even more structured in the mixture, while the least structured distribution will shift in the opposite direction. This behavior is found for PEP, hhPP, and PEB. The PEP/PEP distributions in Figure 4a are all enhanced, as all materials with which PEP is mixed are less structured than itself. The size of the enhancement depends on the difference in pure component packing. When PEP is mixed with hhPP, the material with packing most similar to itself, very little change in $g^{inter}(r)$ is observed. On the other hand, mixing with PP, which packs quite differently, causes a significant enhancement in the PEP/PEP distribution. The position of the peak in $g^{inter}_{PEP/PEP}(r)$ does not change, which indicates that the preferred separation distance for neighboring chains of PEP is unaltered with mixing. Rather, the number of united atoms separated by this distance relative to the bulk density is increased. The overall picture is thus that a larger fraction of PEP chains are located at the characteristic separation distance from PEP neighbor chains in the blends than in the pure state. Examining Figure 4b, the hhPP/hhPP distribution is suppressed in PEP, a more efficient packer, has little change in PEB, with which it is very similar, and is enhanced in PP, a less efficient packer. The response of the PEB/PEB distribution (Figure 4c) to the environment is similar: packing is enhanced in PP, a less efficient packer, and suppressed in PEP, a more efficient packer. The trend is not followed for PEB in hhPP, where the packing of neighboring PEB chains is enhanced, despite the fact that hhPP is a more efficient packer and athermal mixing would suggest it should decrease. Again, the behavior of PP (Figure 4d) is different, with the PP/PP distribution enhanced when mixed with two out of the three blend partners [hhPP and PEB], although PP is the least efficient packer of the group.

We now consider the behavior of the cross-distribution. In Figure 6, we consider each blend in turn, with the A/A, B/B, and A/B distributions plotted, along with the A/A and B/B distributions in pure A and in pure B. For example, Figure 6a addresses the PEB/PEP blend, with the PEB/PEB, PEP/PEP, PEB_{pure}/PEB_{pure}, PEP_{pure}/PEP_{pure}, and PEB/PEP distributions plotted. An athermal mixture would be characterized by a cross-distribution that is an arithmetic or geometric mean of the other two. This is the case in Figure 6a [PEP/PEB] and Figure 6b [PP/PEP]. For the PEP/PEB blend, this behavior extends throughout the spatial range of the

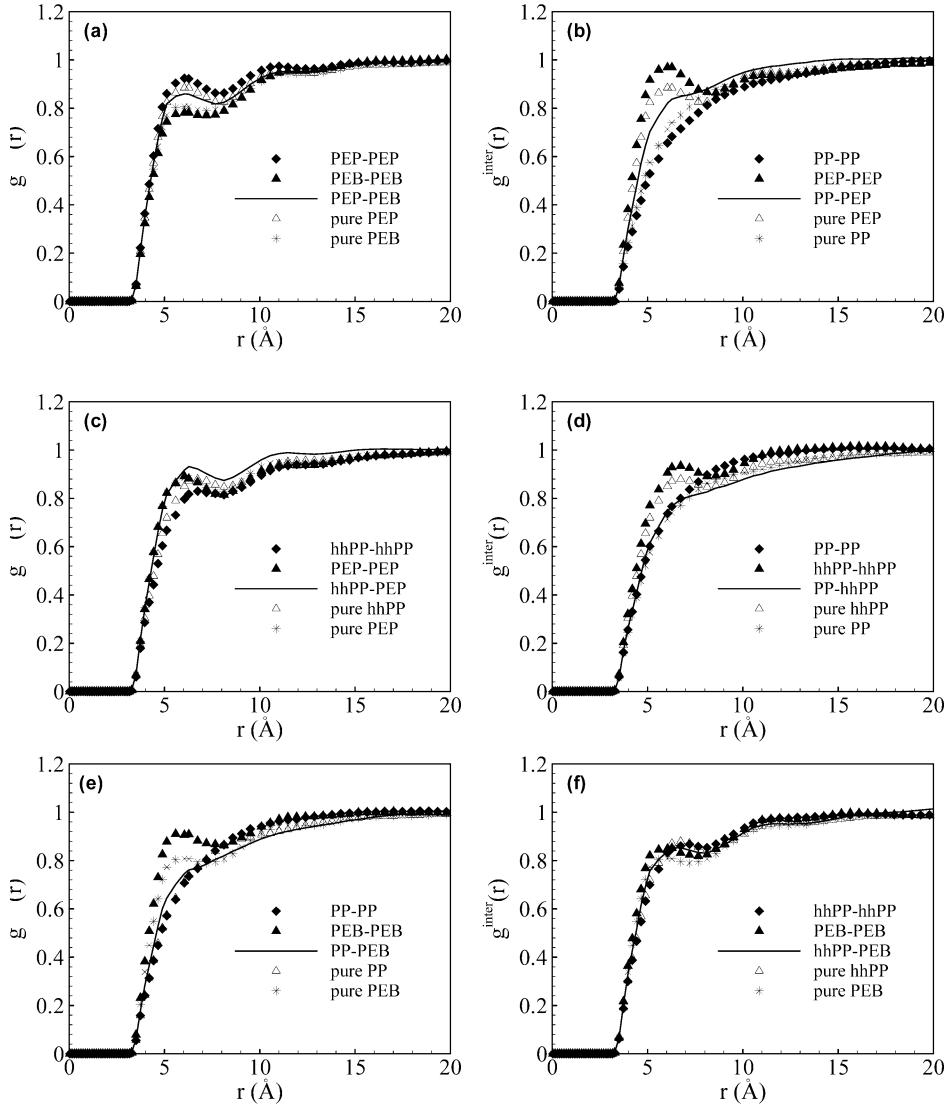

Figure 6. Intermolecular packing characteristics of each blend. A/A, A_{pure}/A_{pure}, B/B, B_{pure}/B_{pure}, and A/B intermolecular pair distribution functions are shown. (a) PEP−PEB, (b) PP−PEP, (c) hhPP−PEP, (d) PP−hhPP, (e) PP−PEB, and (f) hhPP−PEB. Symbols are as in the figure legend.

calculation, where for PP/PEP athermal behavior is noted until ∼9 Å, which is near the R_g of both components. Before 9 Å, the cross-distribution is an average of the two self-distributions, such that the distance for neighboring A/B contacts is a function of the "thickness" of each chain. The placement of nearest PEP and PP segments occurs at a distance intermediate between the more highly branched PP chain [larger effective thickness] and the less branched PEP chain [smaller effective thickness]. After 9 Å, the distribution no longer reflects the local packing of neighboring chains, but rather the relative placement of the chains' center of mass. Here there are more cross-contacts [PEP/PP] than either of the self-contacts, which would indicate that there is a slight preference for adjacent placement of opposite, over same chains in this blend. On examining the results for the other four blends, this behavior, where a shift in the cross-distribution occurs near R_g, is observed for all blends containing PP. In the other two, PP/hhPP (Figure 6d) and PP/PEB (Figure 6e), the cross-distribution becomes less than both self-distributions above R_g.

Illustrated in Figure 6c is a blend [hhPP/PEP] with enhanced cross-distributions over the entire spatial range. Both local and center of mass packing are increased. The origin of this enhanced local packing, as well as the A/B packing of the other blends, can be rationalized on the basis of the local chain architectures of the components. First, both components have the same size [methyl as opposed to ethyl] side groups. In addition, the space between consecutive methyl groups on the PEP chain is just large enough to accommodate the two consecutive methyl groups on the hhPP chain without crowding them. Figure 7 illustrates one potential combination of local A/B chain architectures for each blend we have considered. The figure is meant to depict a segment of an A chain that packs next to a segment of a B chain for one to two repeat units. The situation is simplified in that all of the backbone bonds are in the trans configuration—the dominant configuration in these systems. The order in which the blends appear is the same as in Figure 6. The enhanced A/B contacts of the hhPP/PEP blend are indicated with the uncrossed arrow. In the case of hhPP−PEP, segments of the two chains are able to approach each other closely without undue interference from side groups. The methyl group on PEP is ∼4 Å in size [the σ value in the LJ potential], and the space between side group clusters on hhPP is

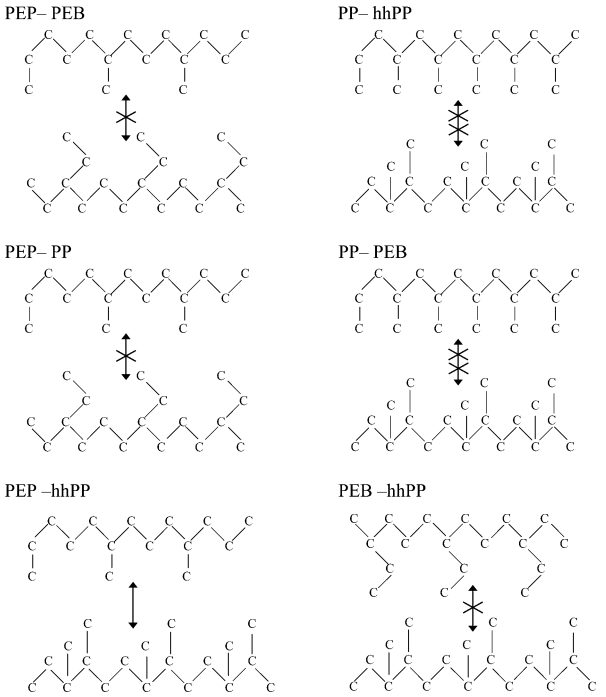

Figure 7. Schematic illustration of adjacent A/B packing in all blends.

∼3.5 Å [based on bond length of 1.54 Å and equilibrium bond bending angle]. A single X on the arrow indicates blends with A/B distributions that are near averages. In these cases, the two chains can fit together, but at closest packing of backbones, the two sets of side groups are closer than is optimal—in the PP−PEP blend, there is ∼2.5 Å between side groups on PP to accommodate the PEP side group. In contrast, the combination of PP with hhPP results in a situation where the local chain architectures simply cannot accommodate one another, indicated by a double X on the arrow. This is reflected in the cross-distribution for this blend (Figure 6d) being suppressed. Similar behavior is found for the PEB/PP blend (Figure 6e), where the combination of the larger ethyl side group in PEB and the lack of consecutive carbons without methyl groups on the backbone of PP lead to difficulty in local packing. When PEB is mixed with hhPP, rather than PP, where two consecutive undecorated backbone carbons are available, the cross-distribution again becomes an average. This blend is unique in that all its distributions are very similar. To extend this analysis to the general case, rather than an idealized picture of isolated all trans sequences, we consider the packing of side groups [CH_3 united atoms] on hhPP with branch points [CH groups] on three blend partners with various packing efficiencies: PP [poor], PEB [average], and PEP [enhanced]. This CH_3(hhPP)−CH(X) distribution is shown in Figure 8. The closest packing [first peak] is largest and sharpest for hhPP/PEP, which has enhanced cross-packing, and becomes smaller and broader for hhPP/PEB, which has average packing characteristics. For the poor packing blend, hhPP/PP, the side group is unable to approach the PP backbone in the closest packing region, as evidenced by the absence of a peak. These calculations, which reflect averages over the simulation box and include all types of local sequences, and not just idealized trans sequences, support the ideas presented above, namely, that the origins of enhanced and poor packing lie in the ability of side groups to fit within open sequences on partner chains.

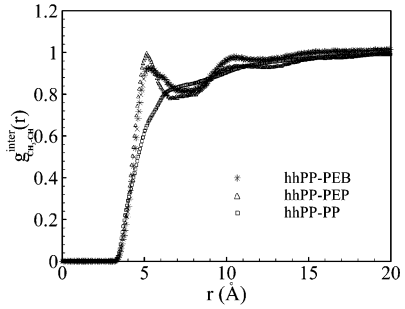

Figure 8. Partial $g(r)$ between the CH_3 united atom on hhPP and the CH united atom on PEP, PEB, and PP.

Table 3. Blend Cohesive Energy Density and the Average [$CED_{ave} = (CED_A CED_B)^{1/2}$] Calculated from the Pure Components for All Mixtures[a]

mixtures	CED	CED_{ave}	mixtures	CED	CED_{ave}
PEP−PEB	216	215	PP−hhPP	190	188
PP−PEP	192	192	PP−PEB	196	193
hhPP−PEP	213	210	hhPP−PEB	213	210

[a] The standard deviation in CED and CED_{ave} is ±2 MPa.

We now consider the possibility that these packing characteristics are energetically driven. Shown in Table 3 are the cohesive energy densities of each blend and the average cohesive energy density $CED_{ave} = (CED_A CED_B)^{1/2}$, where CED_A and CED_B are the cohesive energy densities of the pure components. If the enhancement or suppression of A/B contacts is driven by energetics, then the cohesive energy density of the blend should differ from this average. For all the blends considered here, no energetic gains are found from mixing, within our ability to measure them.

V. Concluding Remarks

These results show that although the overall configuration and local arrangements of atoms *within a chain* are quite insensitive to mixing, the relative placement of *different chains* depends on the nature of the environment. We have changed the environment by mixing with a second component, but one might imagine doing this in other ways: introducing nanoparticles, varying the pressure, or incorporating the chain as a segment in a di- or triblock copolymer of different morphologies. Observed shifts in self-packing [the A/A or B/B distributions in a blend, as compared to the pure component] follow some general trends. The direction of the change is most often such that the two distributions move further apart in the blend: the more structured component packs better, while that with the least structure pack less efficiently. The size of the change is proportional to the difference between the blend components: When the distributions of the two pure components are quite different, the changes are larger. These observations hold in general for PEP, hhPP, and PEB, but the response of PP is unusual. The PP/PP distribution does not change much on blending, although it is the least structured of the four, and in some cases [PEP, hhPP], it is able to increase packing efficiency when blended. PP is the only material that has no indication of a preferred packing distance, i.e., a peak in $g^{inter}(r)$, so perhaps the lack of initial preferred packing alters its response to mixing.

In closing, we note that although a large fraction of the EB copolymer blends we considered [8 out of 10] mix athermally, only 2 of the 6 blends we consider here could be considered athermal, and perhaps only 1 of the 6 [PEP/PEB]. This may have some correspondence with the more frequent success of the solubility parameter formalism for the EB copolymers.[19] The single homopolymer blend that follows this simple theory is the PEP/PEB blend—the same blend that we find is athermal. On the other hand, the two EB copolymer blends that did not show athermal mixing characteristics[20] do follow the solubility parameter formalism.

Acknowledgment. Financial support for this work was provided by the National Science Foundation, Polymers Program: DMR-0134910.

References and Notes

(1) Maranas, J. K.; Kumar, S. K.; Debendetti, P. G.; Graessley, W. W.; Mondello, M.; Grest, G. S. *Macromolecules* **1998**, *31*, 6998.
(2) Maranas, J. K.; Kumar, S. K.; Debendetti, P. G.; Graessley, W. W.; Mondello, M.; Grest, G. S. *Macromolecules* **1998**, *31*, 6991.
(3) Neelakantan, A.; Maranas, J. K. *J. Chem. Phys.* **2004**, *120*, 465.
(4) Richter, D.; Arbe, A.; Colmenero, J.; Monkenbusch, M.; Farago, B.; Faust, R. *Macromolecules* **1998**, *31*, 1133.
(5) Maranas, J. K.; Kumar, S. K.; Debendetti, P. G.; Graessley, W. W.; Mondello, M.; Grest, G. S. *Comput. Chem. Eng.* **1998**, *22*, S19.
(6) Londono, J. D.; Annis, B. K.; Habenschuss, A.; Smith, G. D.; Borodin, O.; Tso, C.; Hsieh, E. T.; Soper, A. K. *J. Chem. Phys.* **1999**, *110*, 8786.
(7) Carlsson, P.; Swenson, J.; Börjesson, L.; Torell, L. M.; McGreevy, R. L.; Howells, W. S. *J. Chem. Phys.* **1998**, *109*, 8719.
(8) Uhlherr, A.; Doxastakis, M.; Mavrantzas, V. G.; Theodorou, D. N.; Leak, S. J.; Adam, N. E.; Nyberg, P. E. *Europhys. Lett.* **2002**, *57*, 506.
(9) Kacker, N.; Weinhold, J. D.; Kumar, S. K. *J. Chem. Soc., Faraday Trans.* **1995**, *91*, 2457.
(10) Han, J.; Boyd, R. H. *Macromolecules* **1994**, *27*, 5365.
(11) Boyd, R. H.; Pant, P. V. K. *Macromocules* **1991**, *24*, 6325.
(12) Pant, P. V. K.; Han, J.; Smith, G. D.; Boyd, R. H. *J. Chem. Phys.* **1993**, *99*, 597.
(13) Curro, J. G.; Weinhold, J. D.; Rajasekaran, J. J.; Habenschuss, A.; Londono, J. D.; Honeycutt, J. D. *Macromolecules* **1997**, *30*, 6264.
(14) Curro, J. G.; Webb, E. B., III; Grest, G. S.; Weinhold, J. D.; Putz, M.; McCoy, J. D. *J. Chem. Phys.* **1999**, *111*, 9073.
(15) Weinhold, J. D.; Curro, J. G.; Habenschuss, A.; Londono, J. D. *Macromolecules* **1999**, *32*, 7276.
(16) Schweizer, K. S.; Curro, J. G. *Adv. Polym. Sci.* **1994**, *116*, 319.
(17) Rajasekaran, J. J.; Curro, J. G. *J. Chem. Soc., Faraday Trans.* **1995**, *91*, 2427.
(18) Krishnamoorti, R.; Graessley, W. W.; Balsara, N.; Lohse, D. J. *Macromolecules* **1994**, *27*, 3073.
(19) Krishnamoorti, R.; Graessley, W. W.; Dee, G. T.; Walsh, D. J.; Fetters, L. J.; Lohse, D. J. *Macromolecules* **1996**, *29*, 367.
(20) Neelakantan, A.; Stine, R.; Maranas, J. K. *Macromolecules* **2003**, *36*, 3721.
(21) Stevenson, C. S.; Curro, J. G.; McCoy, J. D.; Plimpton, S. J. *J. Chem. Phys.* **1995**, *103*, 1208.
(22) Singh, C.; Schweizer, K. S. *J. Chem. Phys.* **1995**, *103*, 5814.
(23) Weinhold, J. D.; Kumar, S. K.; Singh, C.; Schweizer, K. S. *J. Chem. Phys.* **1995**, *103*, 9460.
(24) Jaramillo, E.; Grest, G. S.; Curro, J. G.; Wu, D. T., preprint.
(25) Akten, E. D.; Mattice, W. L. *Macromolecules* **2001**, *34*, 3389.
(26) Clancy, T. C.; Putz, M.; Weinhold, J. D.; Curro, J. G.; Mattice, W. L. *Macromolecules* **2000**, *33*, 9452.
(27) Rajasekaran, J. J.; Curro, J. G.; Honeycutt, J. D. *Macromolecules* **1995**, *28*, 6843.
(28) Jorgenson, W. L.; Madura, J. D.; Swenson, C. J. *J. Am. Chem. Soc.* **1984**, *106*, 6638.
(29) Paul, W.; Smith, G. D.; Yoon, D. Y. *Macromolecules* **1997**, *30*, 7772.
(30) Smith, G. D.; Paul, W.; Yoon, D. Y.; Zirkel, A.; Hendricks, J.; Richter, D.; Schober, H. *J. Chem. Phys.* **1997**, *107*, 4751.
(31) Maranas, J. K. Ph.D. Thesis, Princeton University, 1997.
(32) Mondello, M.; Yang, H. J.; Furuya, H.; Roe, R. J. *Macromolecules* **1994**, *27*, 3566.
(33) Berendsen, H. J. C.; Postma, J. P. M.; Van Gunsteren, W. F.; Di Nola, A.; Haak, J. R. *J. Chem. Phys.* **1984**, *81*, 3684.
(34) Krishnamoorti, R. Ph.D. Thesis, Princeton University, 1994.
(35) Schweizer, K. S.; Singh, C. *Macromolecules* **1995**, *28*, 2063.
(36) Indrakanti, A.; Maranas, J. K.; Kumar, S. K. *Macromolecules* **2000**, *33*, 8865.
(37) Londono, J. D.; Maranas, J. K.; Mondello, M.; Habenschuss, A.; Grest, G. S.; Debenedetti, P. G.; Graessley, W. W.; Kumar, S. K. *J. Polym. Sci., Polym. Phys.* **1998**, *33*, 3001.

MA0303770